

NUMERIC INVESTIGATIONS OF FIELD ELECTRON EMISSION FROM CARBON NANOTUBES

*J. Blažek*¹⁾, *P. Špatenka*²⁾, *Ch. Taeschner*³⁾, *A. Leonhard*³⁾

¹⁾ University of South Bohemia, Department of Physics, Jeronýmova 10,
CZ-371 15 České Budějovice, Czech Republic

²⁾ Technical University of Liberec, Department of Materials Science, Hálkova 6,
CZ-461 17 Liberec, Czech Republic

³⁾ Institut für Festkörper- und Werkstofforschung Dresden E.V., Helmholtzstrasse 20,
D-01069 Dresden, Germany

Carbon nanotubes (CNTs – long tubular carbon nanostructures) belong to the best electron field emitting materials. A code developed in FEMLAB enables numeric investigations of various aspects of field enhancement properties of CNTs. It was shown that there exist an optimum distance of neighboring nanotubes, for which the emitted electron current reaches its maximum, and that the current is strongly sensitive to the shape of the CNTs tips. To verify the reliability of the 3-D FEMLAB modeling we computed field emission characteristics of a conductive sphere placed in a homogeneous electric field and compared them with their theoretical values.

Keywords: FEMLAB, carbon nanotubes, field electron emission

Introduction

Fowler-Nordheim (FN) theory was introduced in 1928 [1]. The electric field above the emitting surface enables the electrons tunneling outward. According to the simplest model, the field emission (FE) electron current density is

$$j = AE^2 \exp\left(-\frac{B}{E}\right) \quad (1)$$

where numerically

$$A = \frac{1.54 \cdot 10^{-6}}{\varphi}, \quad B = 6.83 \cdot 10^9 \varphi^{3/2}. \quad (2)$$

Parameter φ is the work function expressed in eV. For all our computations we assumed $\varphi = 5$ eV.

Therefore, the so-called Fowler – Nordheim plot $\log J / E^2$ versus $1/E$ is linear with a slope of B (see Fig. 1).

The serious problem in the formula (1) arises in connection with the local field E close to the emitter tip, as it cannot be measured directly. It is expressed as $E = \gamma E_0$, where E_0 is the average macroscopic field ($E_0 = U/d$, where U is the voltage between negative substrate and positive electrode and d is their distance) and γ is the field enhancement factor: This coefficient strongly depends on the geometry of the CNTs tips and it is difficult to compute it [2,3].

Computations of FE current from the spherical surface

To verify the numerical reliability of our computations, we tested them first on a conductive sphere placed in a homogeneous field. The field enhancement factor γ of a sphere can be theoretically evaluated [4],

$$\gamma \equiv \frac{E}{E_0} = 3 \cos \theta \quad (3)$$

where θ is the angle between the normal of the surface and the homogeneous field \vec{E}_0 . Hence, the total FE current emitted from the hemisphere of the radius R is

$$I = \pi R^2 18 A E_0^2 \int_0^{\pi/2} \exp\left(-\frac{B}{3 E_0 \cos \theta}\right) \cos^2 \theta \sin \theta \, d\theta. \quad (4)$$

After some computations one obtains the average current density emitted from the surface

$$\langle j_{\text{theor}} \rangle \equiv I / \pi R^2 = 2 A B^2 \cdot F(3 E_0 / B), \quad (5)$$

where the function F is defined as follows:

$$F(x) \equiv \frac{\int_0^x \exp(-1/x) x^2 \, dx}{x} \quad (6)$$

Theoretical solutions (5) for various intensities were compared with numerical solutions obtained in FEMLAB, see Tab.1. As is seen from this table, the computations are in agreement with theoretical predictions within the relative error of about 20%. The computational errors come mainly from only two iterations used in the adaptive solver, as three or more iterations would exceed the memory limitation of 512 MB in our computer. Another source of errors originates from boundary condition $\vec{E} \rightarrow \vec{E}_0$ for $r \rightarrow \infty$, which is from computational reasons approximated by the condition $\vec{E} = \vec{E}_0$ on the boundaries of a large box (in this case of the size $7R$) surrounding the sphere.

For FE current emitted from CNTs ellipsoidal tips one can expect an error of the same order as for the spherical surface.

E_0	$\langle j_{\text{theor}} \rangle$	$\langle j_{\text{comp}} \rangle$
1	3.03	3.72
3	38.3	45.8
5	114	136

Tab.1 Comparison of theoretical values of FE current emitted from spherical surface with values computed by FEMLAB. Geometrical units.

Field emission properties of CNT films

Carbon nanotubes [5] are long graphitic cylinders, usually of several nanometers in diameter and of the height of several micrometers. The macroscopic electric field enhanced at their tips

causes cold emission of electrons. These field emission properties of CNTs offer promising technological applications, i.e. in flat panel displays [6].

By the code developed in FEMLAB various aspects of FE properties of CNTs tips can be investigated numerically. The basic form of this command – line function is listed in the Appendix.

Fig. 1 plots current density $j \equiv I/d^2$ (I ... current per one nanotube, d ... distance between neighboring nanotubes) versus macroscopic intensity E_0 . We suppose nanotubes of the height 50 nm, closed with spherical tips of the radius $R = 20$ nm and placed at the distances $d = 70$ nm each from other. For these geometrical parameters the maximum field enhancement factor γ is about 2.5. As the emitted current strongly depends on the electric field, there exists only a narrow range of intensity suitable to technological applications. For chosen geometry and for the work function $\phi = 5$ eV the optimum intensity is of the order of 10^9 V/m.

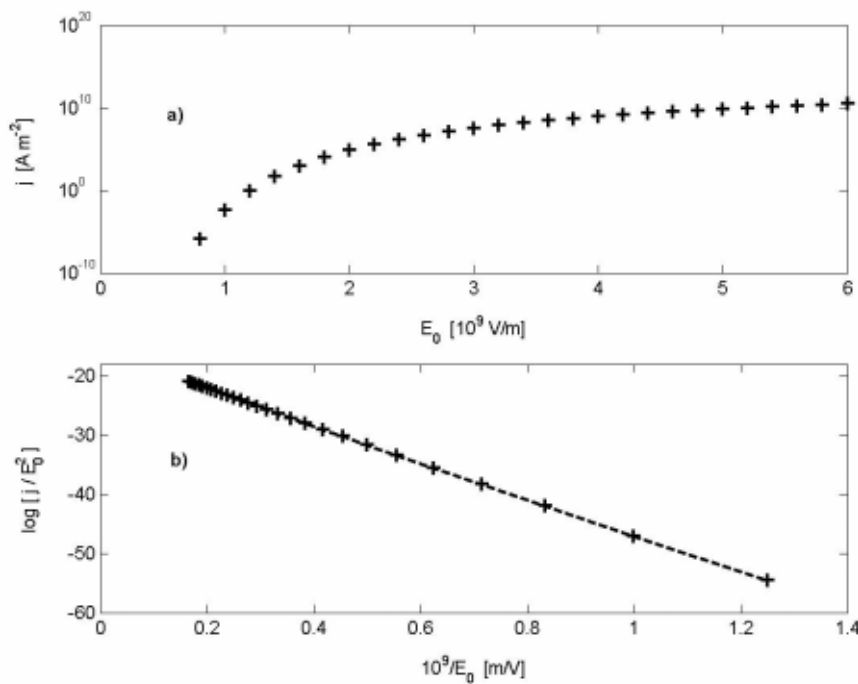


Fig. 1 a) Current density versus electric intensity
b) Fowler – Nordheim plot

In computations of the field enhancement factor the screening effect arising from neighboring nanotubes has to be taken into account. The screening effect is inversely proportional to the distances of the neighboring nanotubes. For high-density film the emission from one nanotube is low whereas the density of CNTs emitters is high. On the contrary, for low-density film the emission from one tip is high and the density of emitters is low. Hence, there exists an optimum distance of CNTs, for which the electron current density reaches its maximum. This effect was experimentally established and theoretically explained in [7]. We investigated this effect numerically. Fig.2 shows the current I emitted from one tip as a function of the distance d between nanotubes. This figure illustrates that from some distance the screening of the neighboring nanotubes becomes negligible, the field enhancement factor reaches its maximum and the current is saturated. Fig. 3 depicts the macroscopic current

density $j = I / d^2$ (current per unit of area) versus the distance. For large distances the current density drops as $1/d^2$.

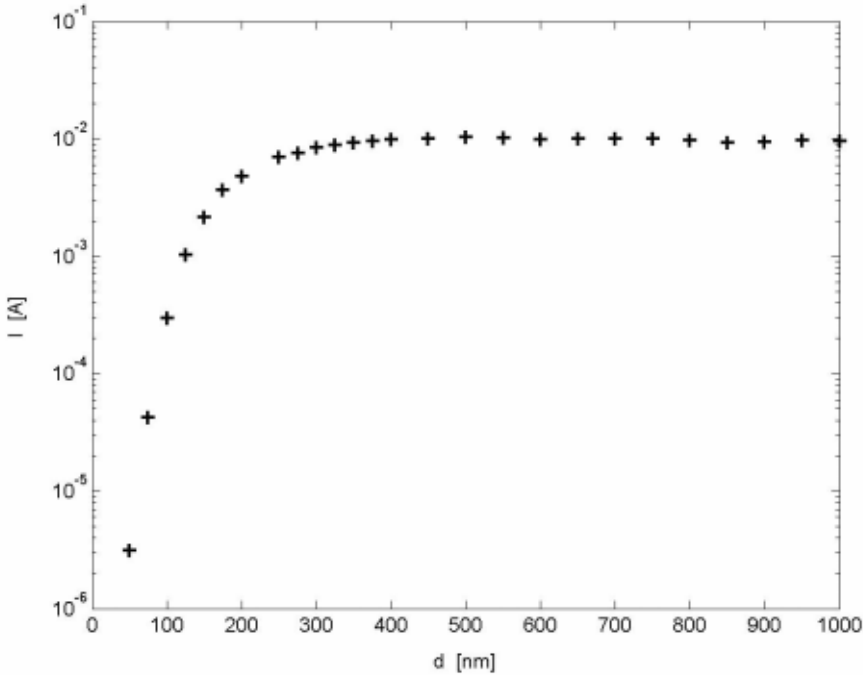


Fig. 2 Current per one nanotube vs. distance; macroscopic intensity $E_0 = 5 \cdot 10^9$ V/m.

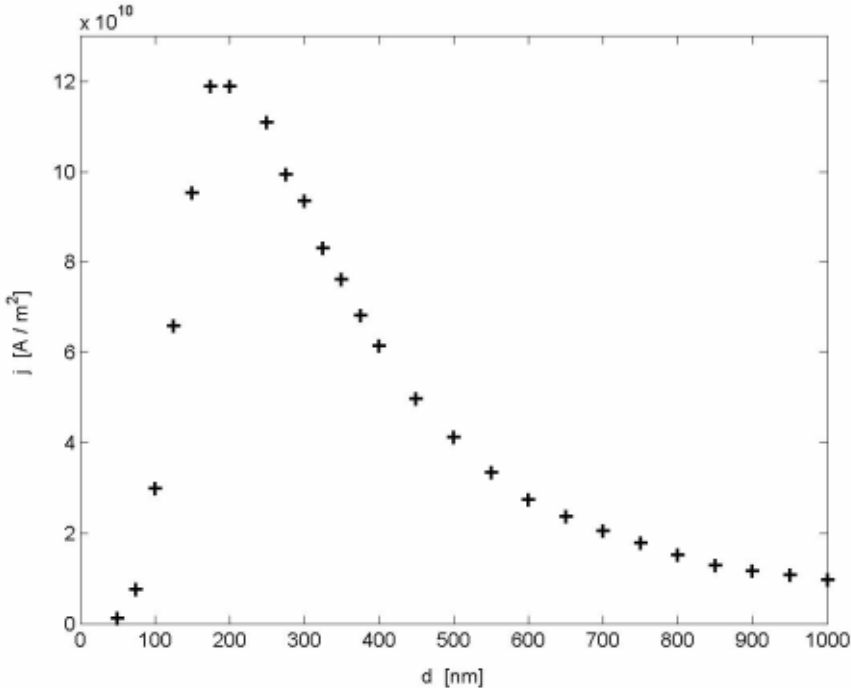


Fig. 3 Current density vs. distance; macroscopic intensity $E_0 = 5 \cdot 10^9$ V/m.

As is shown in Fig.4, the FE current is strongly sensitive to the shape of the CNTs tips. In the computational model we supposed that the nanotube tip is a hemi-ellipsoidal surface[8], characterized by the ratio $k = c/R$, where c and R are the axial semi-axis and radius of the nanotube, respectively. For lower intensities the FE current is more sensitive to the shape of the emitting area than for larger ones. This phenomenon can be probably explained by the existence of an effective emission area. For stronger field the emission area is approximately constant and equal to the whole hemi-ellipsoidal surface. For lower field the emission current density is significant only at some vicinity of the apex, where the local intensity exceeds some threshold value. Hence, the increase of the parameter k is accompanied by increase of both the local field and emitting area and the emission current changes more rapidly.

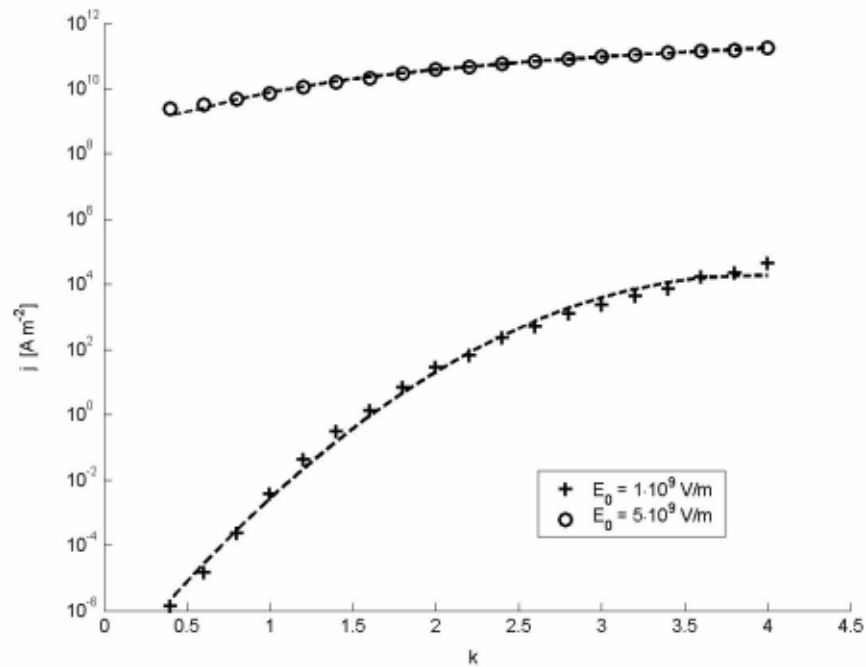


Fig. 4 Dependence of the current emitted from one nanotube with the ellipsoidal tip on the ratio $k \equiv c/R$, where c is the vertical semi-axis and R is the nanotube radius.

The existence of the transition region for the intensity, related to the emission area properties, was also clearly established in the model of a sphere, placed in the homogeneous field. Fig. 5 depicts the dependence of the fraction $I(r)/I(R)$ on the ratio r/R for various macroscopic intensities E_0 . Here $I(r)$ is the FE current emitted from the cross section πr^2 , $0 \leq r \leq R$, and $I(R)$ is the total current emitted from the whole hemisphere of the radius R . As is obvious from the figure, the transition intensity for this model is about 10^9 (arbitrary units). The distribution of the probe current for lower intensities qualitatively differs from the distribution for larger intensities.

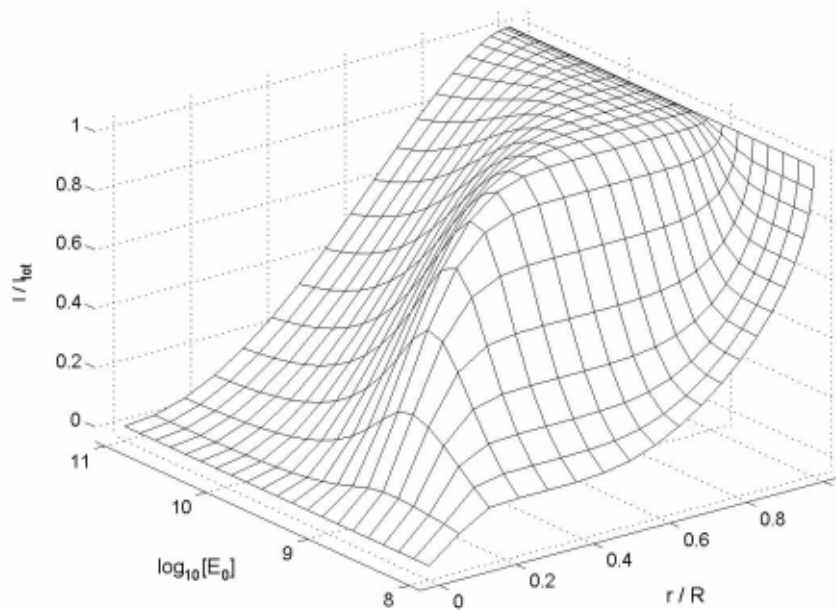


Fig. 5 Relative current $I(r) / I(R)$ emitted from the cross section of radius r from the spherical surface of radius R

Appendix:

FEMLAB command-line function solving FE current from nanotube tip (simplified model)

```
% rNT ... radius of nanotube in nm
% kNT ... semiaxis c/R
% vNT ... height of nanotube
% dNT ... distance between nanotubes
% default values
if ~exist('rNT') rNT = 20; end
if ~exist('kNT') kNT = 1; end
if ~exist('vNT') vNT = 50; end
if ~exist('dNT') dNT = 70; end
cc = [rNT kNT vNT dNT];
cc = input(['\nparametries rNT kNT ...
vNT dNT (' , ...
num2str(cc,'%2g %2g %2g %2g'),') : ','s');
cc = str2num(cc);
var = {'rNT','kNT','vNT','dNT'};
for i = 1:length(cc)
    eval([var{i} ' = cc(i);']);
end
if dNT < 2*rNT
    fprintf('Neni d > 2r !\n\n');
    break;
end

fprintf('\n\nrNT = %5.2f ...
kNT = %4.1f vNT = %5.2f ...
dNT = %6.2f\n', rNT,kNT,vNT,dNT);

% height of the geometry
hNT = vNT + 8*kNT*rNT;

% Field emission, F - N theory
% j = a/Fi * E^2 * exp[-b Fi^(3/2) / E]
% a = 1.541434*1e-6 A eV V^(-2)
% b = 6.830890*1e9 eV^(-3/2) V m^(-1)
a = 1.541434e-6;
b = 6.830890e9;
Fi = 5;
aFi = a/Fi;
bFi = b*Fi^(3/2);

% due to the symmetry only 1/4
% of geometry is evaluated
box = block3(dNT/2,dNT/2,hNT);
tube = cylinder3(rNT,vNT,[0 0 0]);
% droplet as rotational ellipsoid
droplet = ...
ellipsoid3(rNT,rNT,kNT*rNT,[0 0 vNT]);

% fem structure
clear fem;
% E0 ... macroscopic intensity
% E0 = 1 => gama = E/E0 = 1

% U0 ... potential of CNTs
fem.variables = {'U0',0,'E0',1};
fem.geom = box - (tube + droplet);
fem.mesh = meshinit(fem);
fem.mesh = meshsmooth(fem);
% 3d electrostatics mode
appl.mode = flpdees3d;
% faces
% lateral sides of the box: 1 2 8 9
% upper and lower side of the box: 7 4
% side of the tube: 6
% sides of the droplet: 3 5
% 1st group: V = U0, type V
% 2nd group: nD = 0, type nD0
% 3rd group: nD = eps0*E0, type nD
% side:      1 2 3 4 5 6 7 8 9
appl.bnd.ind = [2 2 1 3 1 1 1 2 2];
appl.bnd.type = {'V' 'nD0' 'nD'};
appl.bnd.V = {'U0' {} {} };
% eps0 = 1, D = E
appl.bnd.nD = { {} {} 'E0' };
appl.equ.epsilon = 1;
% charge density
appl.equ.rho = 0;
fem.appl = {appl};
fem = multiphysics(fem);

% adaptive solver, 3 iterations
fem = adaption(fem,'Report','on',...
'Stop','on','NGen',3);
% gama = E
gama = 'sqrt(Vx.^2+Vy.^2+Vz.^2)';

% (h1,h2) ... scope of images in z-direction
h1 = 0; h2 = vNT + 4*kNT*rNT;
% gama, vertical plane
figure;
postplot(fem,'SliceData',gama, ...
'SliceXSpacing',[eps 15*eps], ...
'SliceMap','jet', 'SliceBar','on','Cont','on', ...
'BdL',[3 5 6], 'Tridata',gama, ...
'TriMap','bone','TriFaceStyle','interp', ...
'Axis',[0,dNT/2,0,dNT/2 h1 h2], ...
'AxisEqual','on','View',[90 0]);
xlabel('x [nm]');
ylabel('y [nm]');
zlabel('z [nm]');
title('Enhancement \gamma = E / E0');
% gama, horizontal plane
figure;
postplot(fem, 'TriData',gama, ...
'BdL',[3 5 6], 'Cont','on', 'TriMap','jet', ...
```

```

'TriFaceStyle','interp','TriBar','on', ...
'Axis',[0,dNT/2,0,dNT/2 h1 h2],
'AxisEqual','on','View',[0 90]);
xlabel('x [nm]');
ylabel('y [nm]');
zlabel('z [nm]');
title('Enhancement \gamma = E / E0');

% FE current density
j = 'aFi*E0^2*(Vx.^2+Vy.^2+Vz.^2).*...
exp(-bFi./(sqrt(Vx.^2+Vy.^2+Vz.^2)*E0))';
% alternatively j = aFi*(E0*ncu).^2.*
% exp(bFi./(ncu*E0))';

for E0 = [1 5]*1e9
% surface current density j
figure;
postplot(fem, 'TriData','j','BdL',[3 5], ...
'Variables',{'aFi','aFi','bFi','bFi','E0','E0'}, ...

'Cont','on','TriMap','jet', ...
'TriFaceStyle','interp','TriBar','on', ...
'Axis',[0,dNT/2,0,dNT/2 h1 h2], ...
'AxisEqual','on','View',[0 90]);
xlabel('x [nm]');
ylabel('y [nm]');
zlabel('z [nm]');
title(['Current Density, ...
E0 = ',num2str(E0,'%9.2e')]);

% macroscopic current density jS = I/dNT^2
I = 4*posteint(fem,j,'BdL',[3 5], ...
'Variables',{'aFi','aFi','bFi','bFi','E0','E0'});
jS = I/dNT^2;
fprintf(['\nE0 = %9.2e jS = %9.2e A/m2'], ...
E0,jS);
end

```

Acknowledgement:

This work was supported by the projects MSM OC527.60 and MSM 124100004.

References

- [1] R.H. Fowler, L.W. Nordheim: Proc. Roy. Soc. London A19 (1928) 173.
- [2] C.J. Edgcombe, U. Valdre: Solid-State Electronics 45 (2001) 857.
- [3] J.-M. Bonard et al: Diamond and Related materials 11 (2002) 763.
- [4] J. Blažek, P. Špatenka: FEMLAB modeling of electric field and induced electric force acting on carbon nanotube tip in DC plasma sheath. Proc. of the 10th Conference MATLAB 2002, Vol. 1, Prague 7.11. 2002, 32-39.
- [5] C.N.R. Rao et al: Nanotubes. CHEMPHYSICHEM 2001, 2, 78 – 105.
- [6] W.B. Choi et al: Appl. Phys. Lett. 75 (20) (1999) 3129.
- [7] L. Nilsson et al: Appl. Phys. Lett. 76 (15) (2000) 2071.
- [8] R.G. Forbes, K.L. Jensen: Ultramicroscopy 89 (2001) 17.

Contact:

Josef Blažek
Department of Physics, Pedagogical Faculty
University of South Bohemia
Jeronymova 10, 371 15 České Budějovice
Czech Republic
E-mail: bla@pf.jcu.cz

Petr Špatenka
Faculty of Materials Science
Technical University Liberec
Hájkova 6, 461 17 Liberec
Czech Republic
E-mail: petr.spatenka@vslib.cz